properties. The research of the Saharan dust will lead to a significant study in the future when the model will be available to couple with air chemistry, and cloud and precipitation physics. This complete aerosol model would explain hopefully the micro- and macro-physical properties resulting from the complete cycle of aerosol evolutions, and the analysis of the validated fields against observations would help to estimate the effects on clouds, on radiative characteristics (Patterson, Cillette and Stockton, 1977; Carlson and Caverly, 1977), and on visibility.

REFERENCES

Alexander, R. C. and R. L. Mobley, 1976: Monthly average sea-surface temperatures and ice-pack limits on a 1 degree global grid. Mon. Wea. Rev., 104, 143-148.

Carlson, T. N. and R. S. Caverly, 1977: Radiative characteristics of Sahara dust at solar wavelengths. J. Geophys. Res. , 82, 3142.

Davis, M. H., 1972: Collisions of small droplets: Gas kinetic effects. J. Atmos. Sci., 29, 911-915.

Davis, M. H. and J. D. Sartor, 1967: Theoretical collision efficiencies for small cloud droplets in Stokes flow. Nature, 215, 1371-1372.

Espenshade, Jr. E. B., 1970: Goode's World Atlas. 13th Edition, Rand McNally & Company, Chicago.

Gates, W. L., 1976: The numerical simulation of ice-age climate with a global circulation model. J. Atmos. Sci., 33, 1844-1873.

Hocking, L. M., 1959: The collision efficiency of small drops. Quart. J. Roy. Meteor. Soc., 85, 44-50.

Langmuir, I., 1948: The production of rain by a chain reaction in cumulus clouds at temperatures above freezing. J. Meteor., 5, 175-192.

Lee, I. Y. and P. R. Swan, 1977: Transport of contaminants in the planetary boundary layer. Preprints, Joint Conf. on

FINAL REPORT

Theoretical studies of the transport and removal processes of Sahara dust

by

In Young Lee
Robert D. Bornstein (Principal Investigator)

Department of Meteorology
San Jose State University
San Jose, CA 95192

for NASA Grant NCC 2-5

for the period

April 1, 1979 - September 30, 1979

THEORETICAL STUDIES OF THE TRANSPORT AND REMOVAL PROCESSES OF SAHARA DUST

A subsynoptic scale aerosol model has been dveloped during the last six month at Ames Research Center to study the long term fate of the Saharan dust which may play an important role in affecting the climate over the Atlantic and Europe by cooling the atmosphere due to the increase of the earth's albedo or conversely warming the atmosphere due to the enhancement of the greenhouse effect.

The processes controlling the evolution of aerosol particles may be divided into dynamic processes concerned with the motions of air currents and microphysical processes concerned with the growth of the individual particles. If dust particles are introduced into the atmosphere, the particles will be diffused through a certain layer and transported along the air currents. At the 800 mb level over the Atlantic (see Figure 1. Gates, 1976) the dust particles originating from North Africa will be transported west at inland, southwest near African coast and then be transported northwest passing the ridge. However, the situation is quite different at the 400 mb level (see Figure 2. Gates, 1976) at which the particles whose concentration may be quite small will be transported along the westerly jet to Europe and Mid-East.

The main body of the dust clouds may be contained in the convective layer and transported east to reach the eastern coast of North and Central America. The rate of production of the large particles depends on the collision efficiency which depends in turn on the flow of air in which the particles are imbedded and the dynamics of the particles in response to the drag force exerted by

the air (Langmuir, 1948; Pearcey and Hill, 1957; Hocking, 1959; Shafrir and Neiburger, 1963; Davis and Sartor, 1967; Davis, 1972) as well as their coalescence efficiency. Studies have been made in order to parameterize the removal processes due to coagulation and sedimentation.

A transport model has been developed based on the Ames Planetary Boundary Layer Model (Lee and Swan, 1977; Swan and Lee, 1978). The PBL model has been modified to include dust transport in the convective layer. Therefore, the model consists of three layers; mixed layer, convective layer and free atmosphere. The dust primarily blows off the African desert in a westerly direction and the dust layer thickness seems to be controlled by the daytime depth pf the planetary boundary layer over Africa, and remains constant over the ocean. By the addition of a third layer to the model, this convective layer transport can be taken into account.

The results from a preliminary test run are presented in Figures 3 to 6. For this test run, simple initial and boundary conditions were assumed to provide PBL wind as southeasterly with 6 m/sec, sigma value at interface as 0.85 (about 1200 meters above surface), PBL and surface potential temperature as 295 K, potential temperature jump at interface as 10 K, stability in the convective layer as 50 degrees per sigma and vertical gradients of x- and y-component wind as -40 and 40 m/sec per sigma, respectively. These simulated fields which represent the subsynoptic scale motions for 4:00 a.m. of July 15 were obtained after 48 hours of real time simulation in order to pass the transient period. The surface pressure field (Figure 3) shows the topographic features of the target area as well as the mass distribution of air due to the initial southeasterly wind. The vertically averaged parameters of PBL depth, potential temperature and wind are shown in Figures 4 to 6. The wind pattern over ocean was quite uniform with about 5 m/sec, but

the wind over land was channelled, blocked and drained due mainly to the topographic features. The actual simulation of these parameters will be quite different if the initial and boundary values that varies with time and space are introduced.

In order to simulate the real situation as closely as possible, the initial values and the steady state boundary values are provided from various sources of observational and numerical studies (Posey and Clapp, 1964; Espenshade, Jr., 1970; Alexander and Mobley, 1976; Gates, 1976) and these raw data were interpolated and smoothed to fit properly to the coordinate system employed by the model and to the complex terrain of the target area. In Figures 7 and 8, the surface albedo constructed by Posey and Clapp(1964) and the surface heat capacity field constructed accounting the soil properties (Espenshade, 1970) over the target area are shown, respectively. In Figures 9 through 22, the self-explanatory initial fields constructed to fit the model are shown (Gates, 1976; Alexander and Mobley, 1976) for various parameters. The actual simulations using these initial values are not available at this time. However, we can discuss a few interesting features found from them. As expected, the hot and dry spots (Figures 10 and 13) are located over most of Africa. The PBL is shallow over land. In particular it is shallower over Saharan desert. It is quite moist in the PBL (Figure 13) and quite dry in the convective layer (Figure 14). The PBL momentum field (Figures 15 and 16) can be explained considering the surface pressure pattern (Figure 9).

In the future, this model may be exercised extensively to understand various dynamic and physical processes characterising the behavior of the dust and to validate the results against observations. The surface dust inventory, if available, will be used to parameterize the dust flux in terms of mesoscale parameters such as momentum, drag and atmospheric stability and of surface

Applications of Air Pollution Meteorology, Salt Lake City, 392-399.

Patterson, E. M., D. A. Gillette and B. H. Stockton, 1977: Complex index of refraction between 300 and 700 nm for solar aerosols. J. Geoph. Res., 82, 3153-3160.

Pearcey, T. and G. W. Hill, 1957: A theoretical estimate of the collection efficiencies of small droplets. Quart. J. Roy. Meteor. Soc., 83, 77-92.

Posey, J. W. and P. E. Clapp, 1964: Global distribution of normal surface albedo. Geofis. Intern., 4, 33-48.

Shafrir, U. and M. Neiburger, 1963: Collision efficiencies of two spheres falling in a viscous medium. J. Geophys. Res., 69, 4141-4147.

Swan, P. R. and I. Y. Lee, 1979: Meteorological and air pollution modeling for an urban airport. Prepared for the Fourth Symposium on Turbulence, Diffusion, and Air Pollution, Reno, Nevada.

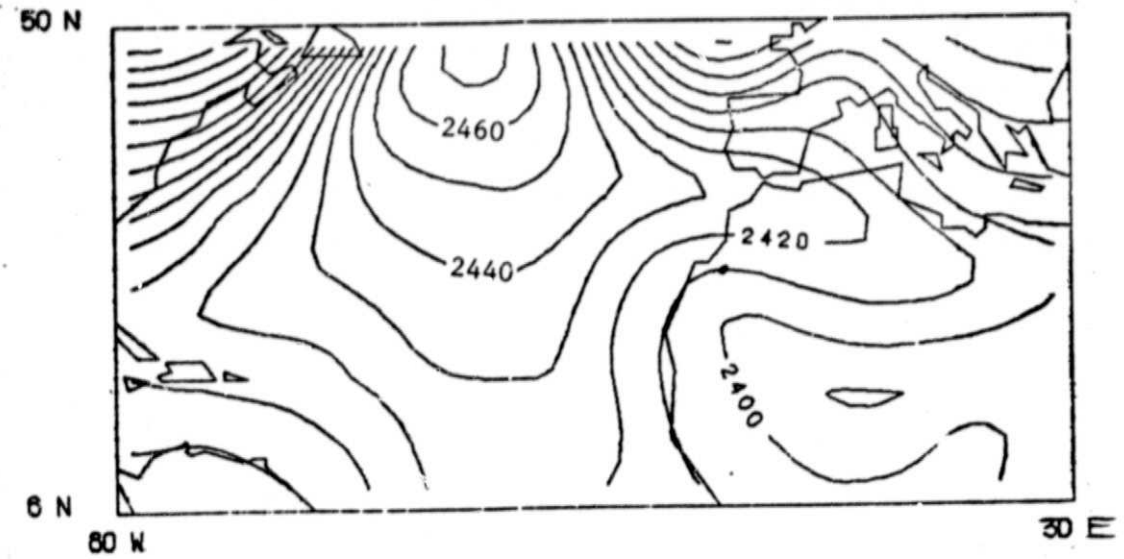

Figure 1. Geopotential Height at 800 mb in meters.

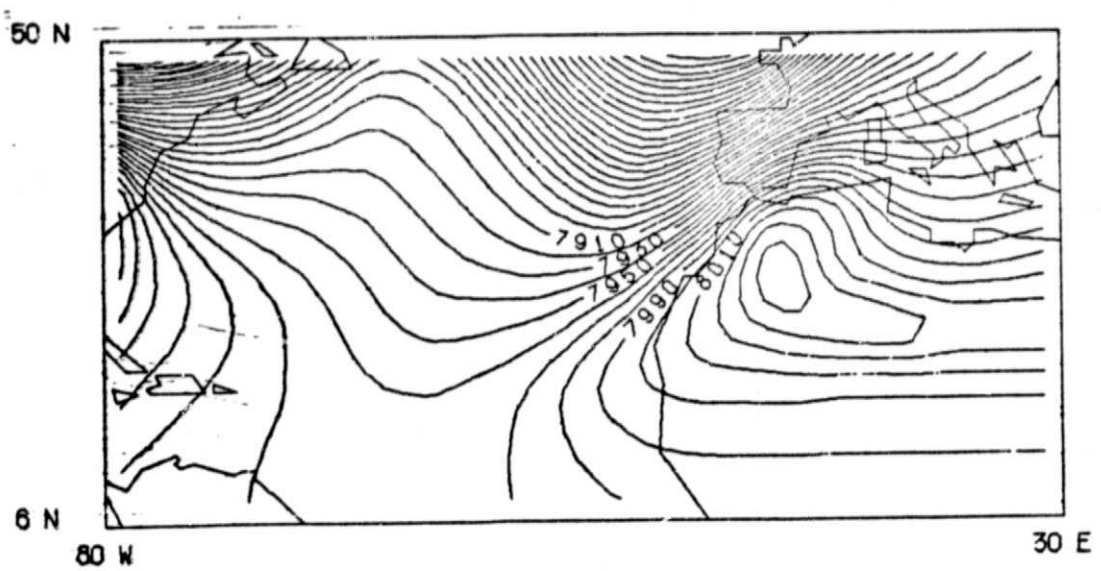

Figure 2. Geopotential Height at 400 mb in meters.

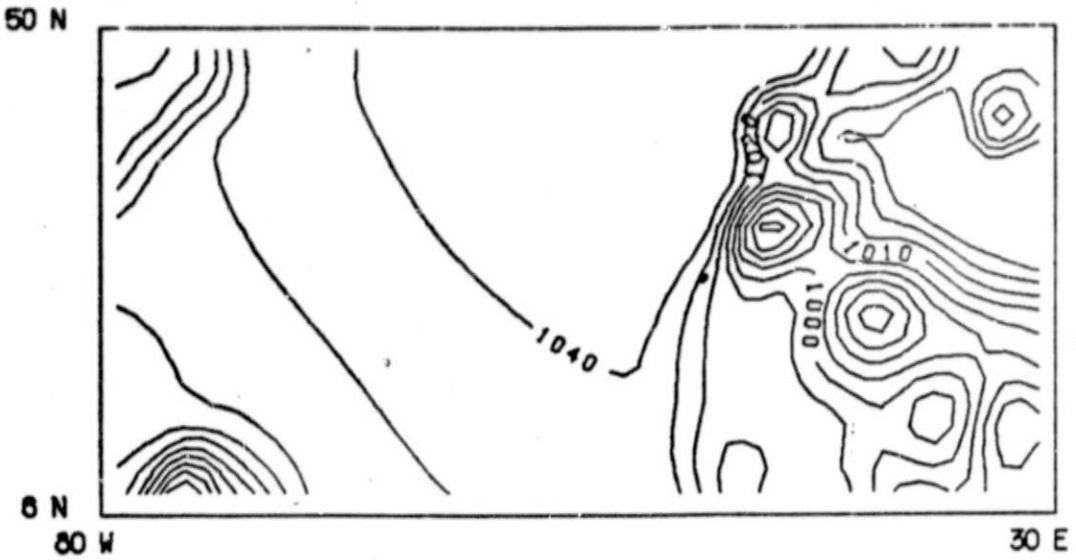

Figure 3. Surface Pressure in mb (Test Run)

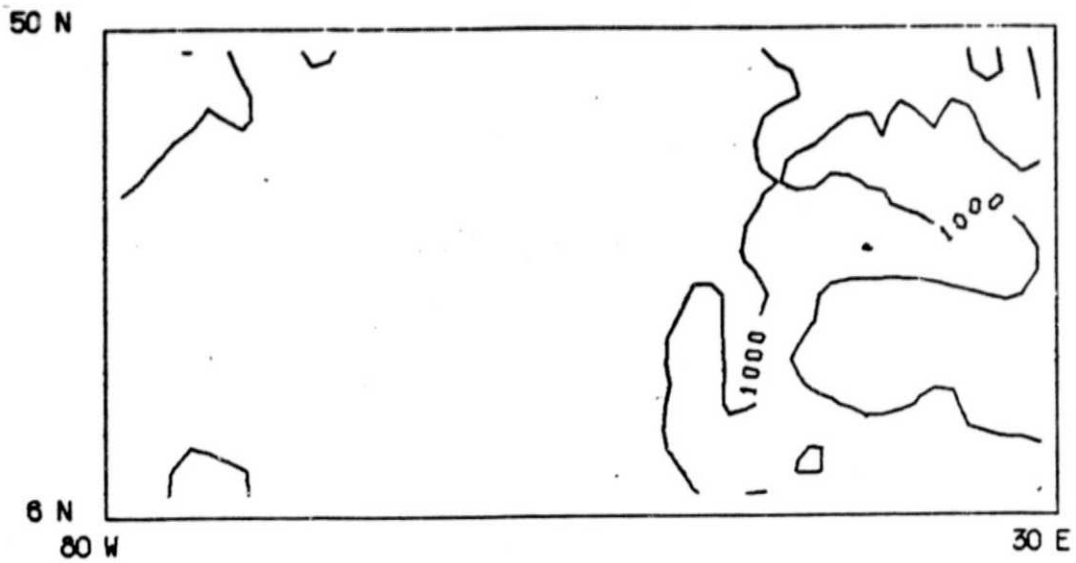

Figure 4. PBL Depth in meters (Test Run)

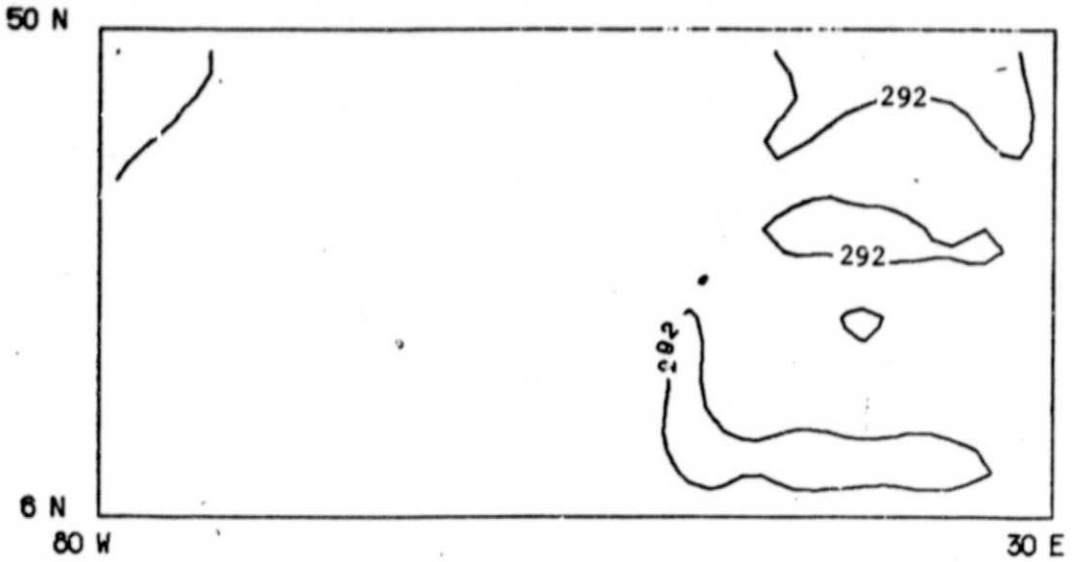

Figure 5. PBL Potential Temperature in K (Test Run)

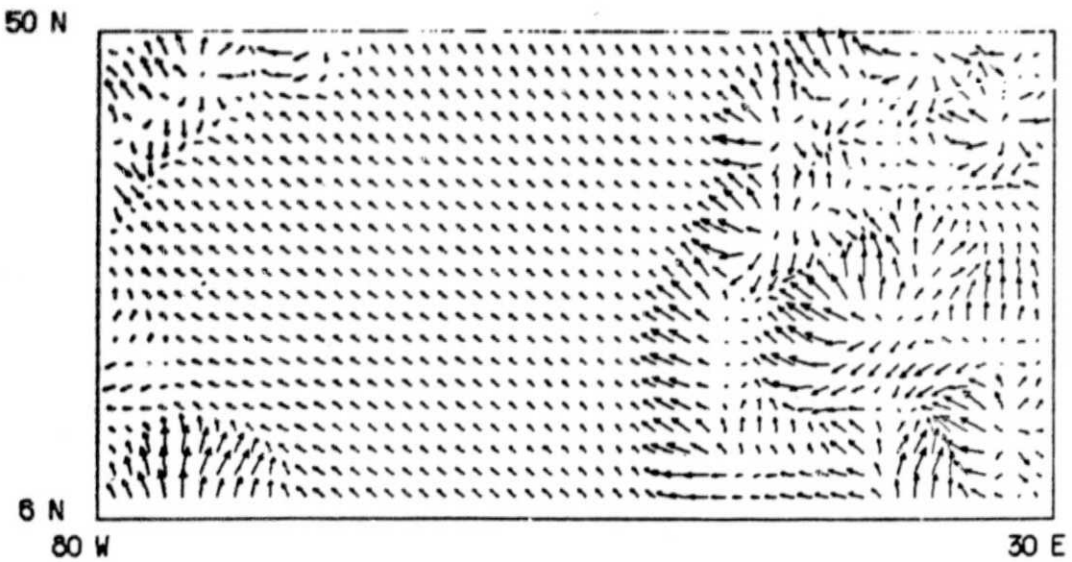

Figure 6. PBL Wind with Maximum 10 m/sec (Test Run)

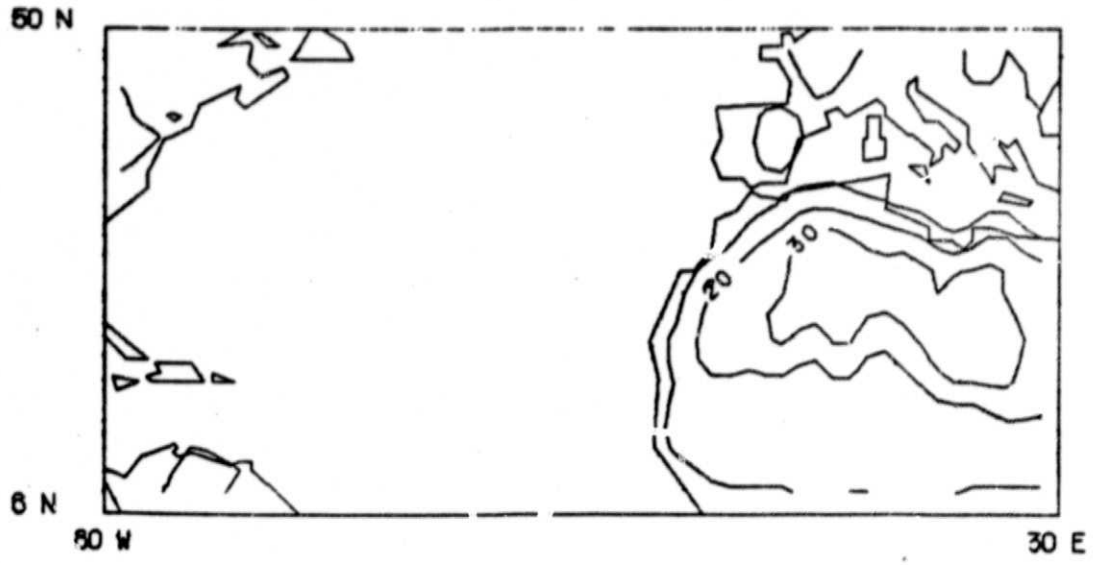

Figure 7. Surface Albedo in %.

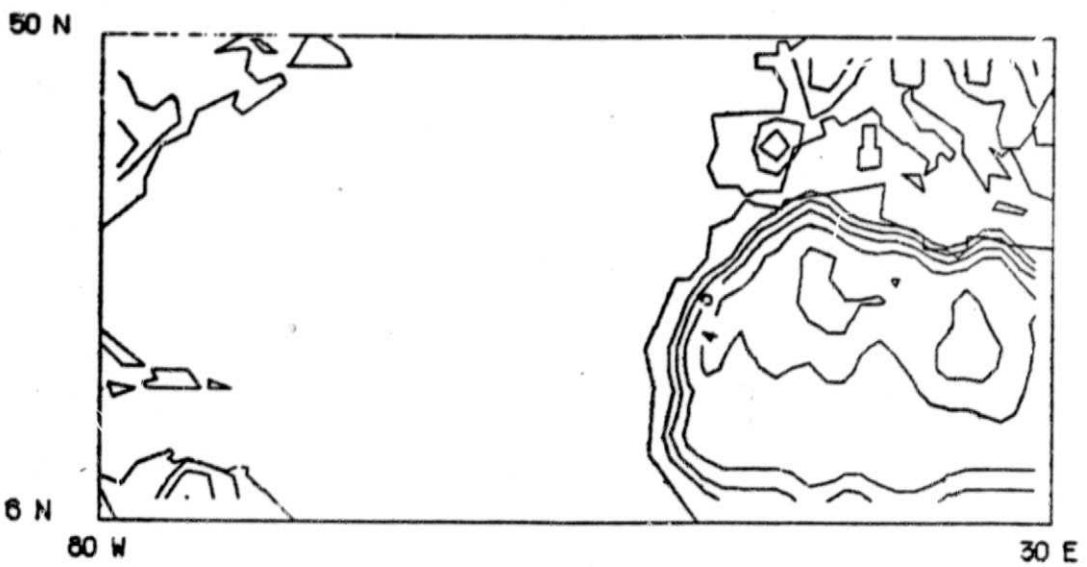

Figure 8. Surface Heat Capacity in cal/cm^2/deg.

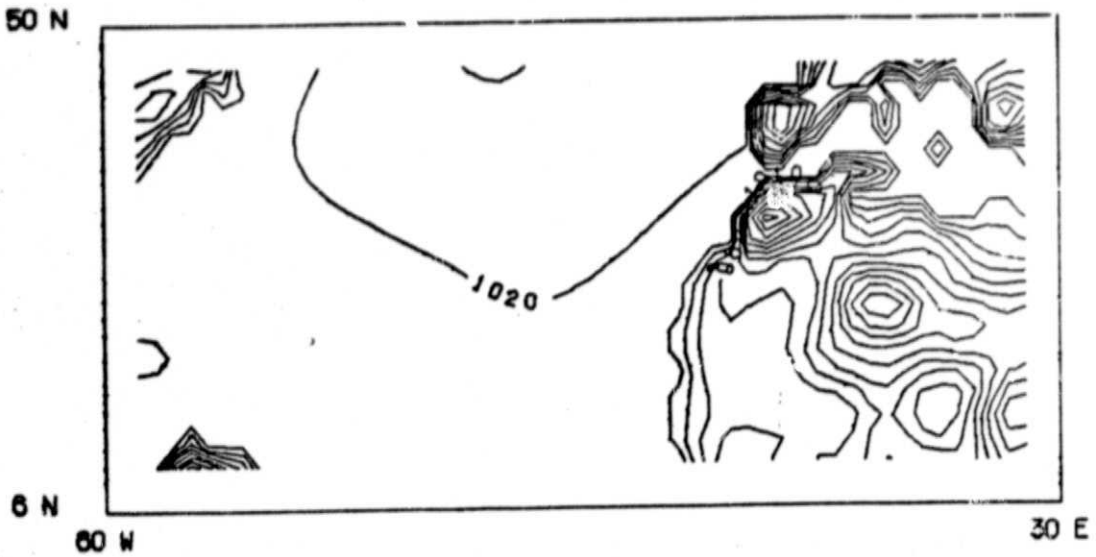

Figure 9. Surface Pressure in mb.

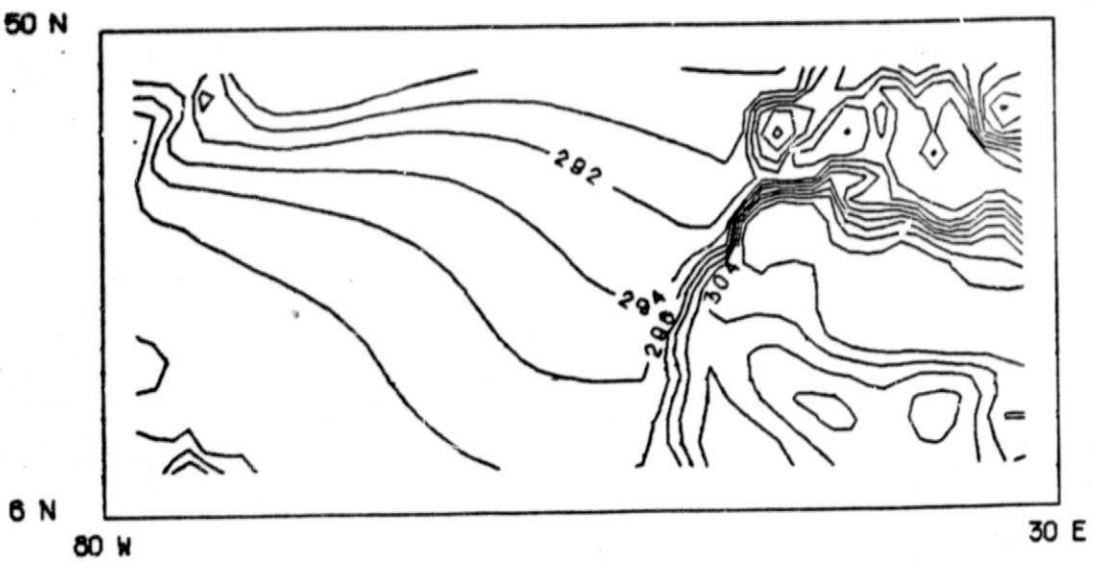

Figure 10. Surface Potential Temperature in K.

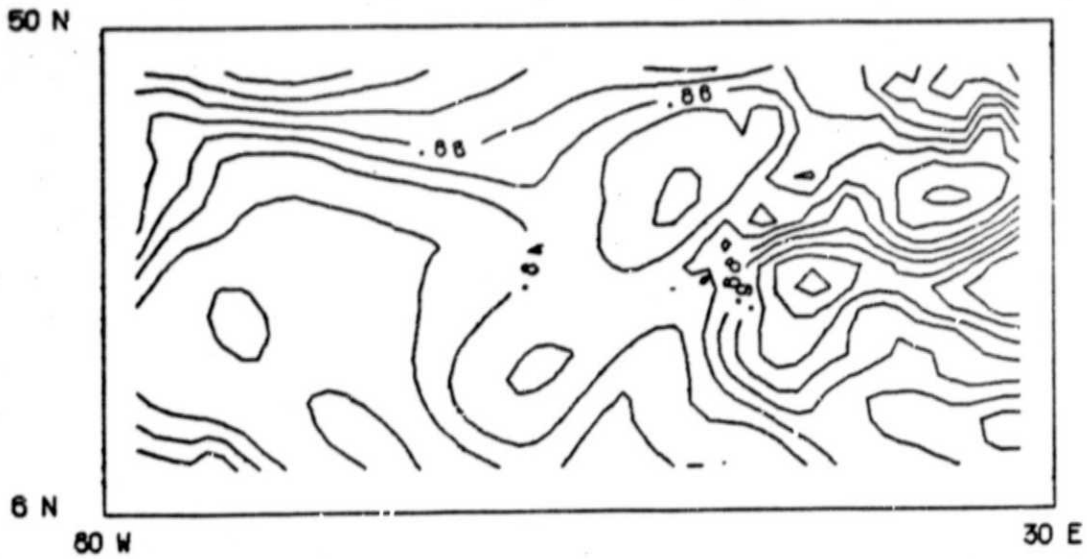

Figure 11. Sigma Value at Interface.

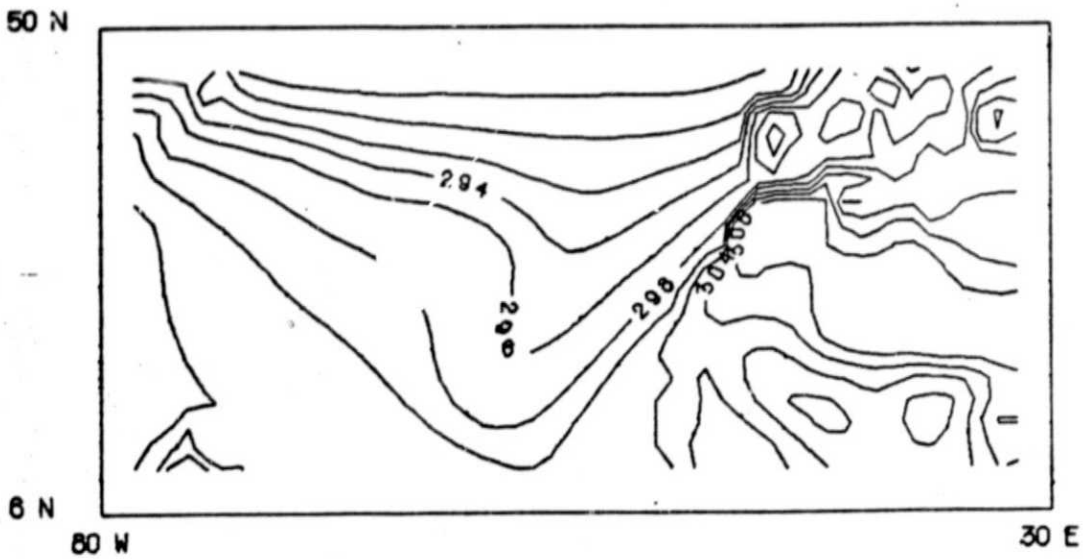

Figure 12. PBL Potential Temperature in K.

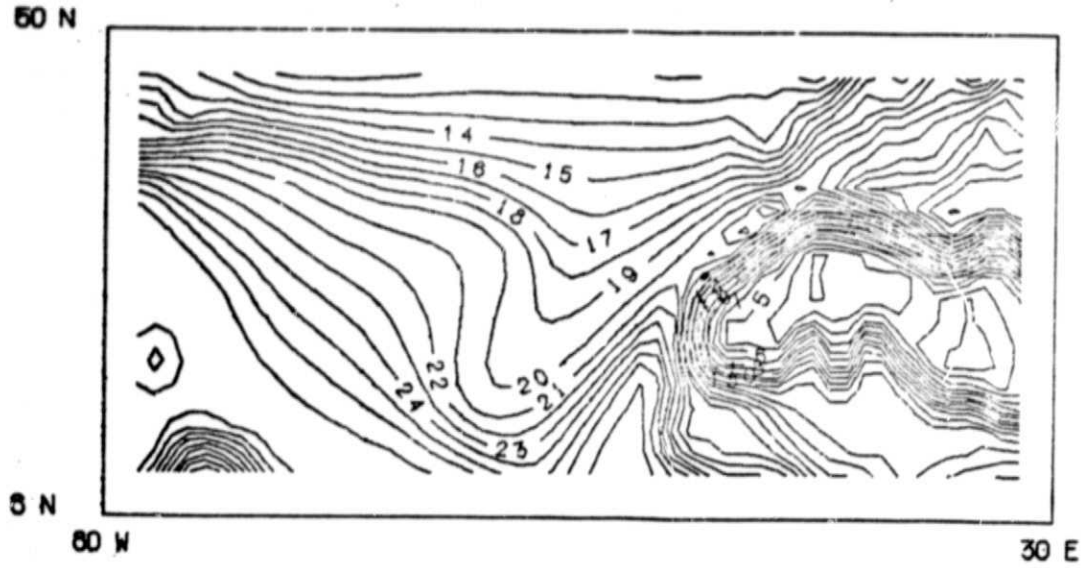

Figure 13. PBL Water Vapor Mixing Ratio in g/kg.

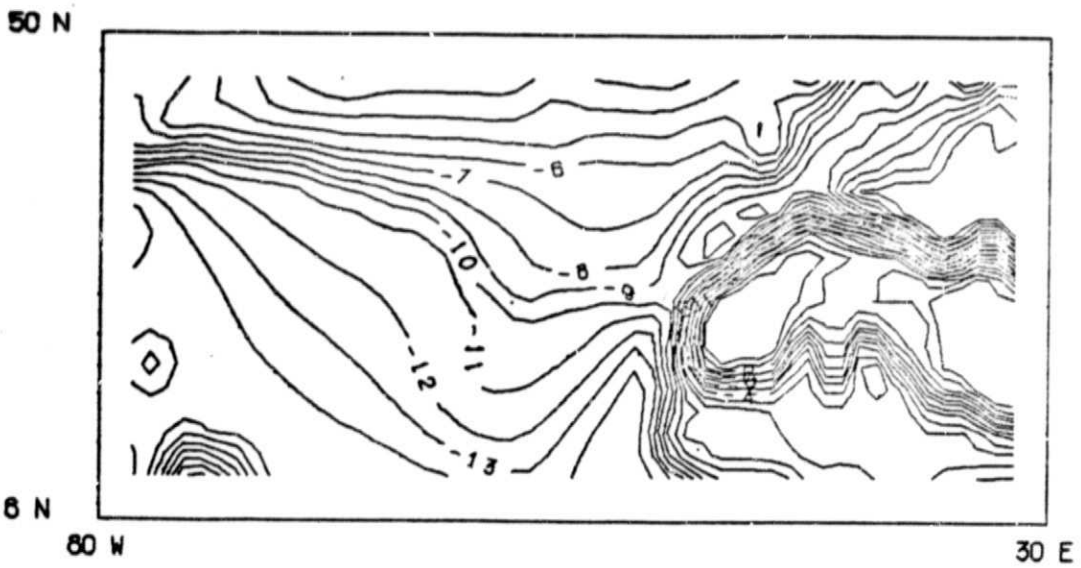

Figure 14. Moisture Drop at Interface in g/kg.

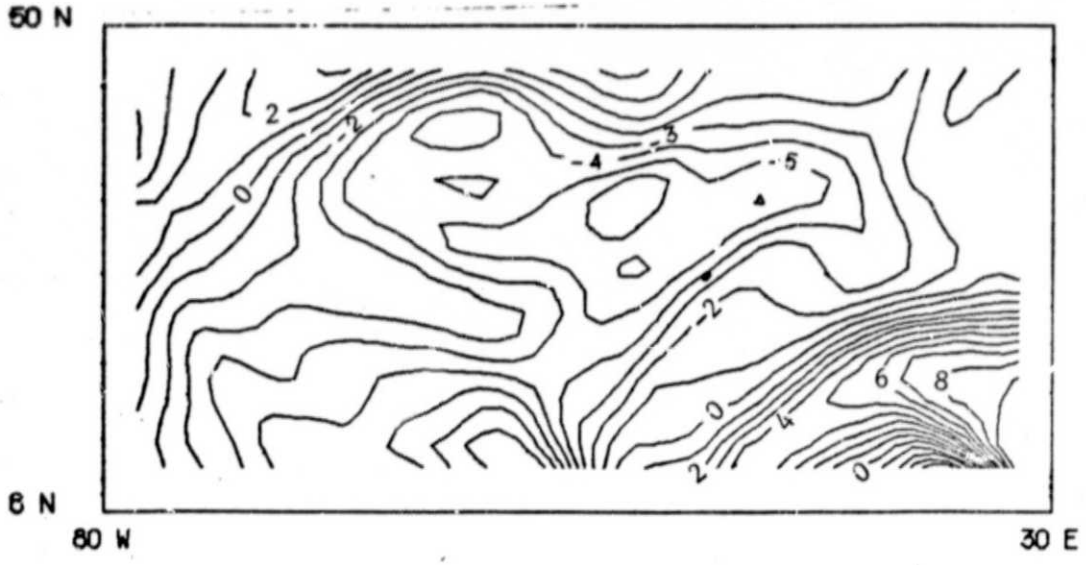

Figure 15. PBL X-Component Wind in m/sec.

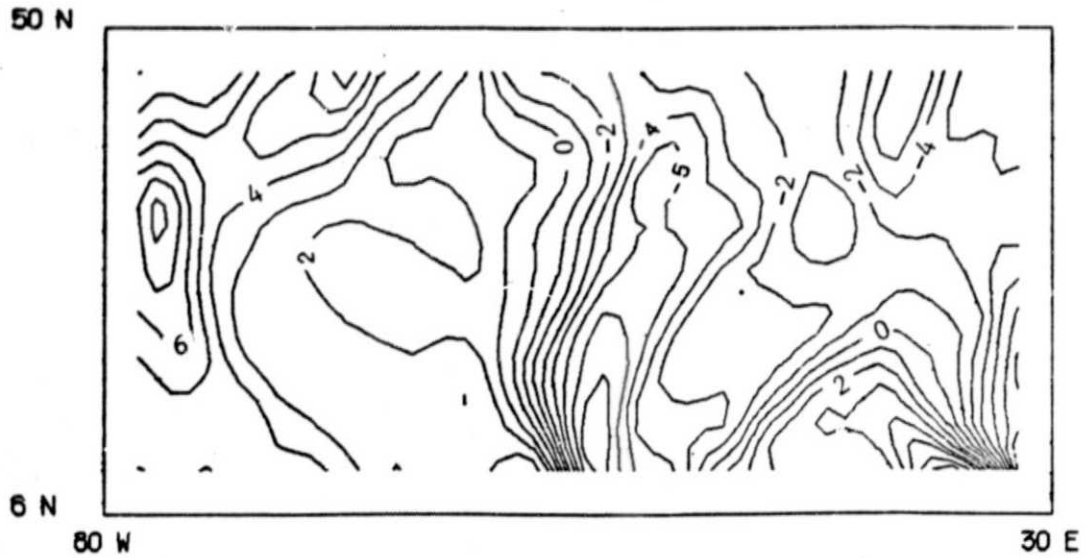

Figure 16. PBL Y-Component Wind in m/sec.

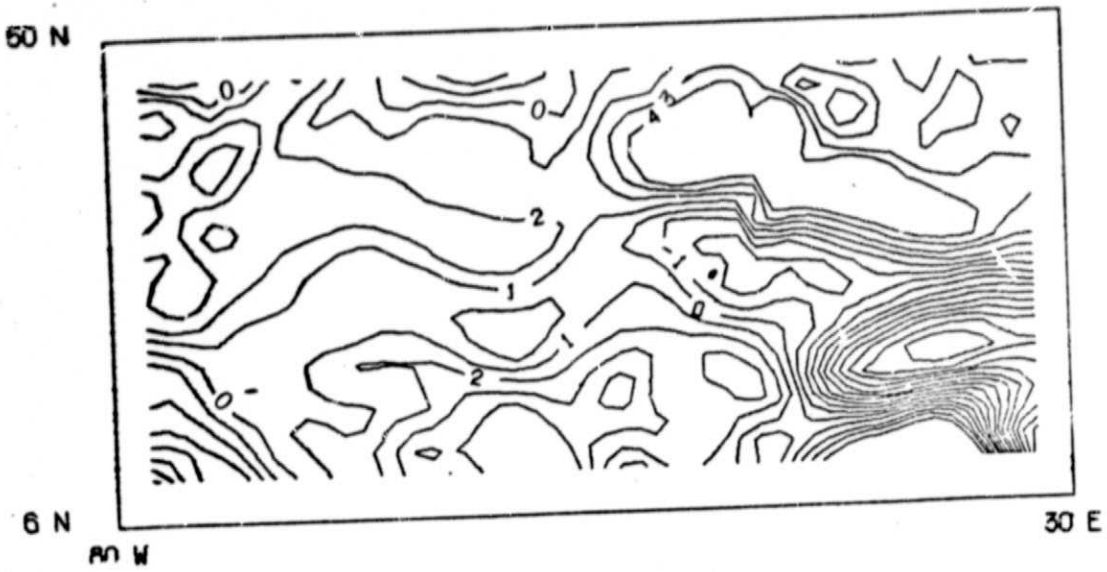

Figure 17. X-Component Wind Jump at Interface in m/sec.

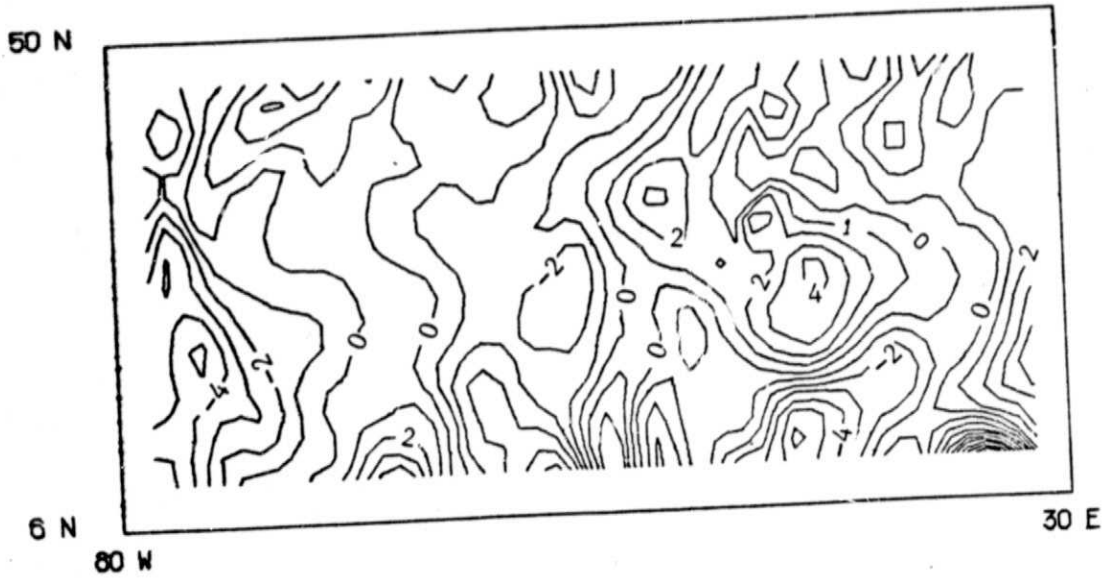

Figure 18. Y-Component Wind Jump at Interface in m/sec.

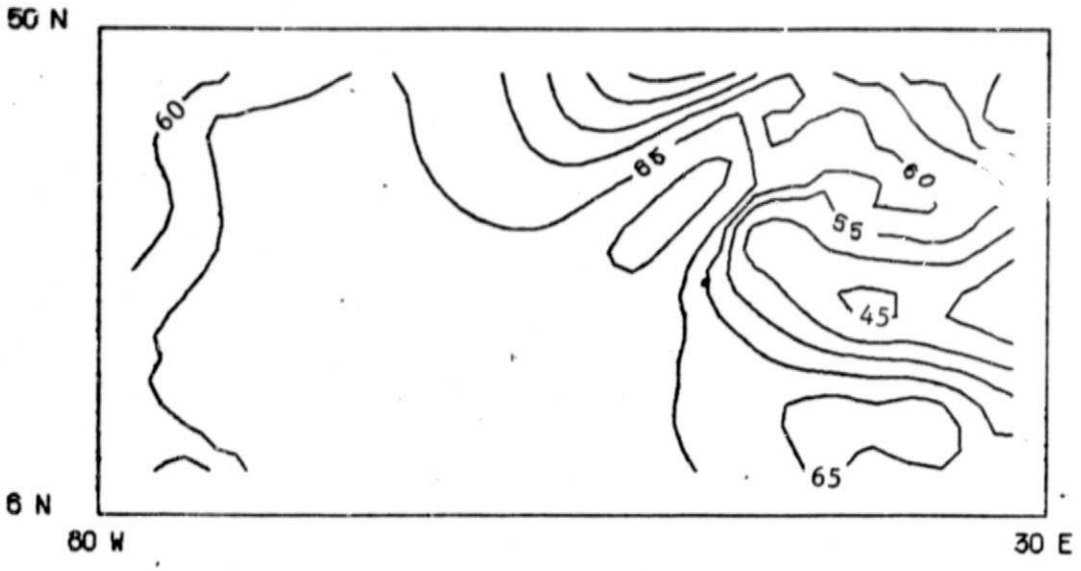

Figure 19. Stability in Convective Layer in deg/sigma.

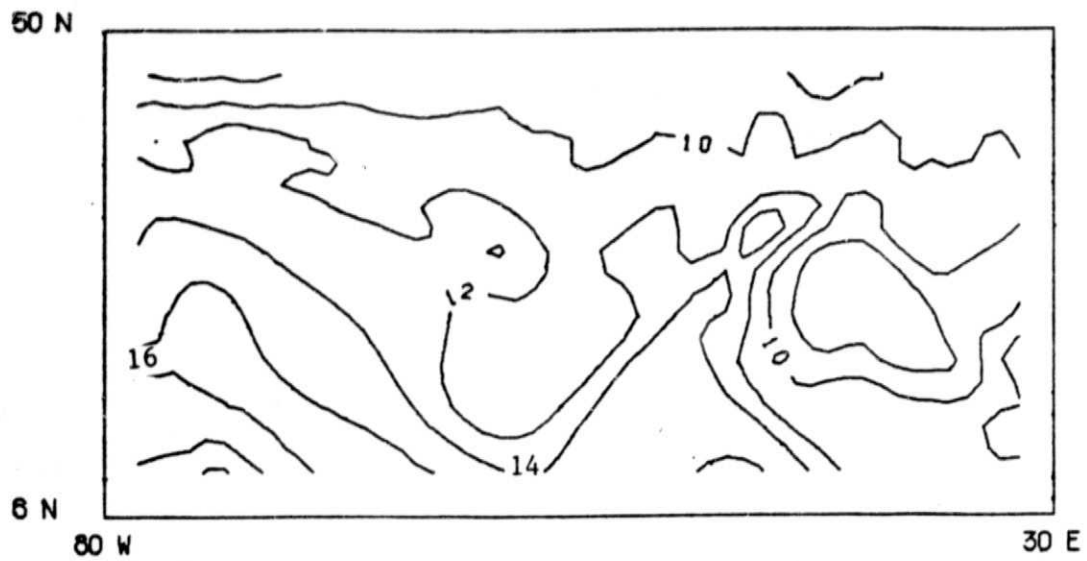

Figure 20. Vertical Gradient of Moisture in g/kg.

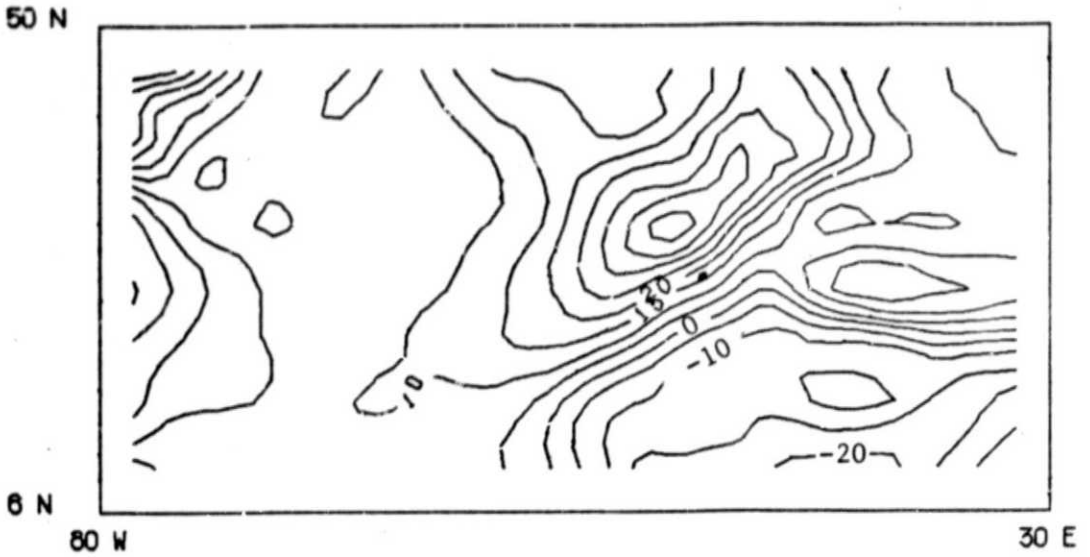

Figure 21. Vertical Gradient of U in Convective Layer in m/s/sigma.

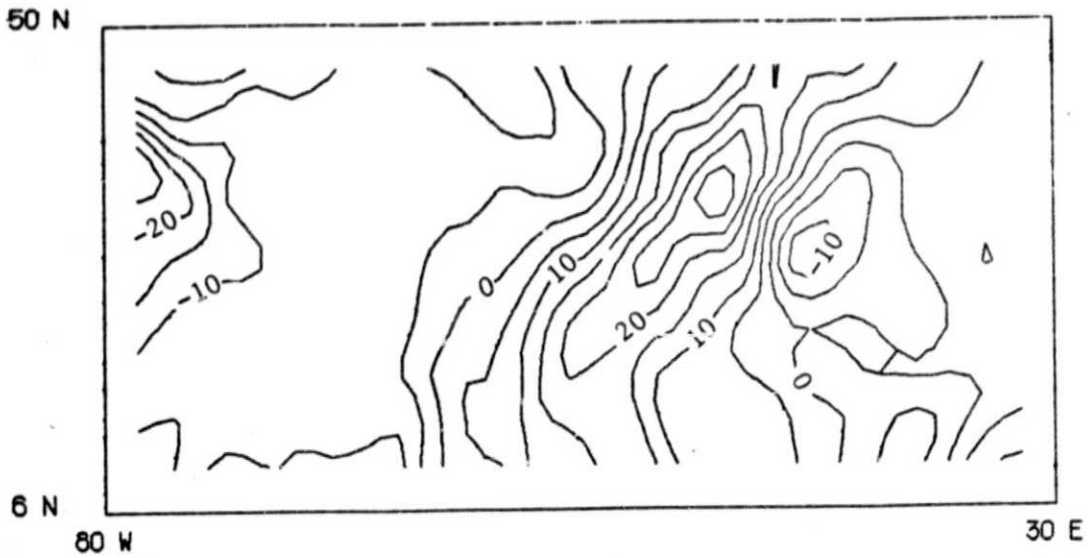

Figure 22. Vertical G lient of V in Convective Layer in m/s/sigma.